Fast recognition of a Digital Straight Line subsegment: Two algorithms of logarithmic time complexity

Isabelle Sivignon

Fast recognition of a Digital Straight Line Subsegment: two algorithms of logarithmic time complexity

Isabelle Sivignon[1]

GIPSA-*lab, CNRS, UMR 5216, F-38420, France*

Abstract

Given a Digital Straight Line (DSL) of known characteristics (a, b, μ), we address the problem of computing the characteristics of any of its subsegments. We propose two new algorithms that use the fact that a digital straight segment (DSS) can be defined by its set of separating lines. The representation of this set in the $\mathbb{Z}^2$ space leads to a first algorithm of logarithmic time complexity. This algorithm precises and extends existing results for DSS recognition algorithms. The other algorithm uses the dual representation of the set of separating lines. It consists of a smart walk in the so called Farey Fan, which can be seen as the representation of all the possible sets of separating lines for DSSs. Indeed, we take profit of the fact that the Farey Fan of order n represents in a certain way all the digital segments of length n. The computation of the characteristics of a DSL subsegment is then equivalent to the localization of a point in the Farey Fan. Using fine arithmetical properties of the fan, we design a fast algorithm of theoretical complexity $\mathcal{O}(\log(n))$ where n is the length of the subsegment. Experiments show that our algorithms are also efficient in practice, with a comparison to the ones previously proposed by Lachaud and Said [1]: in particular, the second one is faster in the case of "small" segments.

Keywords: Digital geometry, Digital straight segment recognition, subsegment, local convex hull, Farey fan

1. Introduction

Digital Straight Lines (DSL) and Digital Straight Segments (DSS) have been known for many years to be interesting tools for digital curve and shape analysis. The applications range from simple coding to complex multiresolution analysis and geometric estimators (see for instance [2] for a recent example). All these applications require to solve the so called DSS recognition problem. Many algorithms, using arithmetics [3], combinatorics [4] or dual-space [5] have been

Email address: `isabelle.sivignon@gipsa-lab.grenoble-inp.fr` (Isabelle Sivignon)

[1]This work has been partially supported by the French *Agence Nationale de la Recherche* (Grant agreement ANR-11-BS02-009)

proposed to solve this problem, reaching a computational complexity of $\mathcal{O}(n)$ for a DSS of length n (see also [6] for an overview).

When no further information is known, all these algorithms are actually optimal. They at the same time decide if the set of grid points is a DSS and compute its characteristics (minimal in some sense). However, we sometimes know beforehand that the set of grid points is a DSS: the algorithm does not need to decide anymore and we can hope for a sublinear-in-time recognition algorithm. For instance, this extra information may come from the knowledge of the characteristics of a DSL containing the set of grid points. This occurs for example in [7] where the multiresolution geometry of a digital object is considered. Another example concerns the digitization of a straight segment on a grid of given size: we know that the set of grid points is a DSS, but its characteristics may be much smaller than the ones of the input straight segment (and not greater than the grid size).

In [7], the authors introduce the following problem: given a DSL of known characteristics and a subsegment of this DSL, compute the minimal characteristics of the DSS. The authors present two algorithms (SmartDSS and ReversedSmartDSS) to solve this problem in [7, 8, 1]: both use the decomposition into continuous fractions of the DSL slope and reach a logarithmic complexity.

However, a deeper search in the state-of-the-art shows that this problem is not so new. Indeed, in [9], the author presents a quick sketch of a method that solves it using the Farey Fan. The announced complexity of the method is $\mathcal{O}(\log^2 n)$ for a segment of length n. Much later, the authors of [10], try to compute the "reduction" of a straight line, which is a simplification of DSL characteristics over a bounded domain. As we will see, this reduction does not compute the minimal characteristics, but the idea is similar.

Our contribution in this paper is to demonstrate that it is possible to solve the DSL subsegment problem in logarithmic time complexity revisiting and deepening the study of the two state-of-the-art algorithms [9] and [10].

The first algorithm is based on the local convex hull algorithm developed in [10] together with the framework for DSS recognition described in [11], but we provide the theoretical results which enable to efficiently compute the minimal characteristics of a subsegment from this hull. The second algorithm, detailed in Section brings the method introduced in [9] up to date: we investigate it further to provide a thoroughly defined algorithm. Moreover, we show how its complexity can be lowered to $\mathcal{O}(\log(n))$ with an astute use of arithmetical properties of the Farey Fan. The latter algorithm was first presented in [12] and a more detailed description is provided here.

Section 2 is dedicated to the presentation of the notions used in this work. Section 3 describes the algorithm based on the local convex hull computation. The algorithm using the dual representation, and more specifically the Farey Fan is detailed in Section 4. At the end of this section, two extensions for slightly different frameworks are presented : in particular, we show that the second algorithm can be directly and reliably applied when the input data is not a DSL but a straight line with non integer parameters. The last section is classically devoted to experimental validations.

2. Preliminary definitions

2.1. Digital line, segment and minimal characteristics

A *Digital Straight Line* (DSL for short) of integer characteristics $(a, b, \mu) \in \mathbb{Z}^3$ is the infinite set of digital points $(x, y) \in \mathbb{Z}^2$ such that $0 \leq ax - by + \mu < max(|a|, |b|)$, with a and b relatively prime [3]. These DSL are 8-connected and often called *naive*. The slope of the DSL is the fraction $\frac{a}{b}$ and $\frac{\mu}{b}$ is the shift at the origin. In the following, without loss of generality, we assume that $0 \leq a \leq b$, such that, on a DSL, there is exactly one pixel for each value of x. In this context, it is easy to see that the set of pixels of a given DSL is defined by a unique triplet (a, b, μ). The remainder of a DSL of characteristics (a, b, μ) for a given digital point (x, y) is the value $ax-by+\mu$. The *upper (resp. lower) leaning line* of a DSL is the straight line $ax - by + \mu = 0$ (resp. $ax - by + \mu = b - 1$). Upper (resp. lower) leaning points are the digital points of the DSL lying on the upper (resp. lower) leaning lines.

A *Digital Straight Segment* (DSS) is a finite 8-connected part of a DSL. It can be defined by the characteristics of a DSL containing it and two endpoints P and Q. However, a DSS belongs to an infinite number of DSLs. In this context, the *minimal characteristics* of a DSS are the characteristics of the DSL containing it with minimal b [13, 1]. Since a DSL is defined by a unique triplet (a, b, μ), the values of a and μ are uniquely defined for a given b, and the minimal characteristics of a DSS are also uniquely defined.

Definition 1 (minimal characteristics). Let $\mathcal{L} = \{(a, b, \mu) \in \mathbb{Z}^3, 0 \leq a \leq b, gcd(a, b) = 1\}$. For a given DSS S, we can define $\mathcal{L}_S = \{L \in \mathcal{L},$ the pixels of S all belong to the DSL of characteristics $L\}$. Let $f : \mathcal{L} \rightarrow \mathbb{Z}$, $f(a, b, \mu) = b$. Then the *minimal characteristics* of S is the triplet $(a_S, b_S, \mu_S) = \arg\min_{L \in \mathcal{L}_S} f(L)$.

Note that the notions of leaning points and lines are similarly defined for DSSs. DSS recognition algorithms aim at computing the minimal characteristics of a DSS, taking profit of the following fact: (a, b, μ) are the minimal characteristics of a DSS if and only if the DSS contains at least three leaning points [3]. In this case, the minimal characteristics are the characteristics of the DSS upper leaning line.

2.2. Minimal characteristics, separating lines and dual space

If we consider the digitization process related to this DSL definition, the points of the DSL $\mathbf{L}$ of parameters (a, b, μ) are simply the grid points (x, y) lying below or on the straight line $l : ax - by + \mu = 0$ (Object Boundary Quantization), and such that the points $(x, y + 1)$ lie above l. We say that $\mathbf{L}$ is the digitization of the straight line l. Note that $\mathbf{L}$ is also the digitization of all the straight lines of equation $ax - by + \rho = 0$ with $\mu \leq \rho < \mu + 1$, where $\rho \in \mathbb{R}$. These lines separate the points X of the DSL from the points $X + (0, 1)$, denoted by $\overline{X}$ (as in [11]), and they are called *separating lines*. Figure 1(a) illustrates the separating lines of a DSL.

A similar set of lines can be defined if a DSS is considered. Let us denote by X the points of the DSS and by $\overline{X}$ the points of the DSS translated by the vector $(0, 1)$. The separating lines are the lines which are above the upper part of the convex hull (upper convex hull for short) of the points X and strictly below the lower part of the convex hull (lower convex hull for short) of the points $\overline{X}$ (see Figure 1 for an illustration). Note that the strict constraint on the lower convex hull makes this definition slightly different from the classical definition in computational geometry. However, geometrically speaking, the set of separating lines is also bounded by the critical support lines of the two convex hulls. We actually have the property that an 8-connected set of grid points is a DSS if and only if its set of separating lines if not empty. This property is used in [11, 14] to design a fast linear in time DSS recognition algorithm. Among the separating lines, the line with integer characteristics (a, b, μ) with minimal b and minimal μ defines the minimal characteristics of the DSS. In the algorithm of [11], the points of the DSS are added one by one and the set of separating lines is updated accordingly, but the minimal characteristics are not extracted.

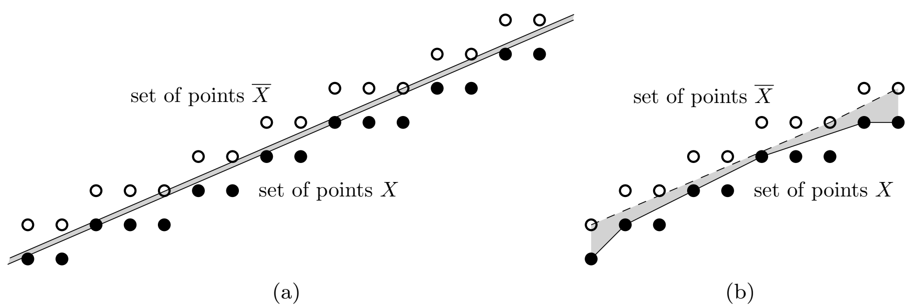

Figure 1: The separating lines of a DSL(a) and of a DSS (b) are the straight lines lying in the gray area.

For a DSS of minimal characteristics (a, b, μ), the structure of the set of separating lines is perfectly known. Indeed, it is defined by the leaning points of the DSS. If U_f (resp. U_l) is the leftmost (resp. rightmost) upper leaning point, and L_f (resp. L_l) the leftmost (resp. rightmost) leaning point, then the set of separating lines is bounded by the lines $(U_f, L_l{+}(0, 1))$ and $(L_f{+}(0, 1), U_l)$ which are the critical support lines, and the lines (U_f, U_l) and $(L_f + (0, 1), L_l + (0, 1))$ which are edges of the lower and upper convex hulls respectively. Figure 2(a) illustrates this structure.

The set of separating lines can also be defined in a dual space, also called parameter space. In this space a straight line $l : \alpha x - y + \beta = 0$ is represented by the 2D point (α, β).

Given a DSS S, a line $l : \alpha x - y + \beta = 0$ is a separating line if and only if for all $(x, y) \in S, 0 \leq \alpha x - y + \beta < 1$. This definition is strictly equivalent to the one given previously. The preimage of S is the representation of the separating lines in the dual space and is defined as $\mathcal{P}(S) = \{(\alpha, \beta), 0 \leq \alpha \leq 1, 0 \leq \beta \leq 1; | \forall (x, y) \in S, 0 \leq \alpha x - y + \beta < 1\}$. As in [9], let us define a ray in this space.

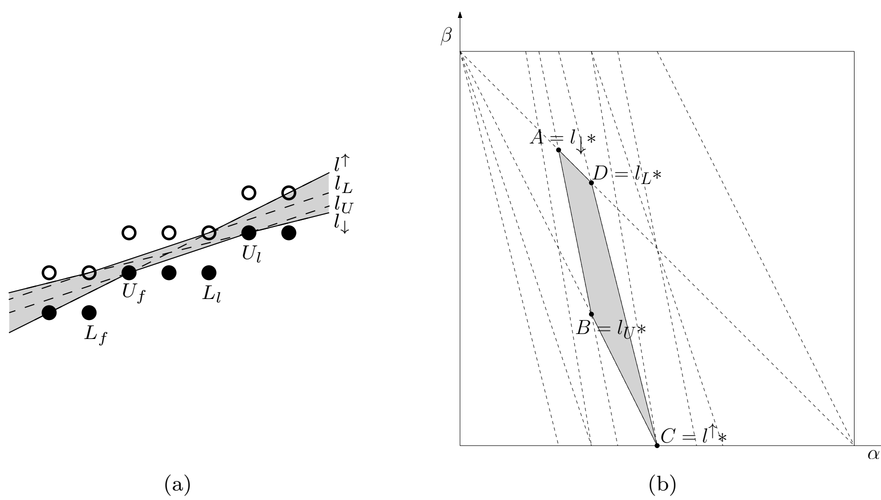

Figure 2: (a) DSS of minimal characteristics $(1, 3, 1)$ with its leaning points U_f, U_l, L_f, L_l. (b) Each vertex of the preimage $\mathcal{P}(S)$ maps to a straight line in the digital space. The vertex $B(\frac{1}{3}, \frac{1}{3})$ maps to the upper leaning line, the characteristics of which are the minimal characteristics of the DSS.

Definition 2 (Ray). Let x and y be two integers. The *ray* defined by x and y is defined and denoted as follows:

$$R(x, y) = \{(\alpha, \beta) | \beta = -x\alpha + y\}$$

x is called the *slope* of the ray.

Note that x is not the geometrical slope of the ray but its absolute value. In the following, the order on the slopes is to be understood as the order on the absolute values of the geometrical slopes.

Given a DSS, any point (x, y) of the DSS induces two linear constraints on the preimage: $\alpha x - y + \beta - 1 < 0$ and $\alpha x + \beta - y \geq 0$. In other words, the preimage is bounded by two parallel rays: it is below the ray $R(x, y+1)$ and above the ray $R(x, y)$.

This definition enables to prove that the preimage of a DSS is a convex polygon with a well-defined structure that is directly related to the leaning points and lines defined by its minimal characteristics [9, 15]. Figure 2 from [16] illustrates this point. In Figure 2(b), all the rays induced by the DSS pixels are depicted as dotted lines. The preimage (in gray) is the intersection of all the constraints bounded by the rays. It is for instance well known that the edges of a DSS preimage are segments of rays induced by the first and last lower and upper DSS leaning points. As a consequence, the preimage of a DSS has either three or four edges. Proposition 1 recalls in detail this specific structure.

Proposition 1 ([16]). *Let $\mathcal{P}(S)$ be the preimage of S. Let $ABCD$ be the polygon defined by this preimage, where A is the upper left most vertex, and the* *vertices are named counterclockwise. Following the notations of Figure 2 we have :*

- *The vertex* $B = l_U*$ *maps to the upper leaning line* (U_f, U_l) *;*
- *The vertex* $D = l_L*$ *maps to the lower leaning line* (L_f, L_l) *translated by the vector* $(0, 1)$ *in the digital space ;*
- *The vertex* $A = l_\downarrow*$ *maps to the straight line* $(U_l, L_f + (0, 1))$ *;*
- *The vertex* $C = l^\uparrow*$ *maps to the straight line* $(U_f, L_l + (0, 1))$.

Note that point B *or* D *may be on the line* (AC). (a, b, μ) *are the minimal characteristics of* S *if and only if* $B = l_U* = (\frac{a}{b}, \frac{\mu}{b})$ *(*a *and* b *relatively prime).* B *is called the* **characteristic point** *of* $\mathcal{P}(S)$.

In the rest of the paper, and especially in Section 4, the edges $[AB]$ and $[BC]$ are called **lower edges**. This dual representation of the set of separating lines has also been used to design DSS recognition algorithms with a linear time complexity [5, 17].

2.3. Statement of the problem

Consider now the following problem:

Problem 1. Given a DSL $\mathbf{L}$ of characteristics $(a_\mathbf{L}, b_\mathbf{L}, \mu_\mathbf{L})$ and two points $P(x_P, y_P)$ and $Q(x_Q, y_Q)$ of this DSL (with $x_P < x_Q$), compute the minimal characteristics (a, b, μ) of the DSS $S = \{(x, y) \in \mathbf{L} \mid x_P \leq x \leq x_Q\}$.

Some easy cases can be withdrawn rapidly (see [8, 1]): if $x_Q - x_P \geq 2b_\mathbf{L}$, then the DSS contains at least three leaning points of the DSL and the minimal characteristics of the DSS are simply equal to $(a_\mathbf{L}, b_\mathbf{L}, \mu_\mathbf{L})$.

For the general case, classical DSS recognition algorithm can obviously be used. But the best complexity of such algorithms is linear in the number of pixels of the DSS. The aim here is to take profit of the extra information given by the DSL that contains the DSS to design a sublinear algorithm. In [8, 1] the authors describe two algorithms of logarithmic time complexity to solve this problem using continued fractions and a top-down or bottom-up path in the Stern-Brocot tree (see for instance [18]). In the following sections, we present two new algorithms of logarithmic time complexity to solve this problem. They use the two representations of the set of separating lines presented in Section 2.2 and illustrated in Figure 2. The algorithm of Section 3 uses properties of the upper and lower local convex hulls (Figure 2(a)) to compute the minimal characteristics, while the algorithm presented in Section 4 takes profit of a strong arithmetical structure (in the dual space, see Figure 2(b)) called Farey fan to solve the problem. The experimental section will show that our algorithms, especially the second one, have a very nice behaviour.

3. Fast computation of local convex hulls

3.1. Rewriting of the problem

Problem 1 can be rewritten as follows:

Problem 2. Given a separating line l of characteristics (a_l, b_l, μ_l) and two bounding abscissas x_P and x_Q such that $x_P < x_Q$, find the line of minimal characteristics that is separating for the same set of points as l for the grid points between x_P and x_Q.

In the following, we denote by X the grid points below l on the interval $[x_P, x_Q]$ such that the points $X + (0,1)$, denoted by $\overline{X}$ are above l. The points X form a DSS by definition.

We present here two properties that show that the minimal characteristics of the DSS can be retrieved from some particular edges of the lower convex hull of $\overline{X}$ and the upper convex hull of X.

Property 1. *Consider the remainder function $r(\alpha, \beta)(x, y) = \alpha x - y + \beta$. Let l be a line of slope α and intercept β that is separating for the DSS S of minimal characteristics (a, b, μ). If the points of S are denoted by X, then the function $r(\alpha, \beta)$ restricted over the points X reaches its smallest positive value for an upper leaning point of S. Similarly, the function $r(\alpha, \beta)$ reaches its greatest value for a lower leaning point of S. Equivalently, if $r(\alpha, \beta)$ is restricted to the points $\overline{X}$, it reaches its greatest negative value for a point $L + (0,1)$ where L is a lower leaning point of S, and smallest value for a point $U + (0,1)$ where U is an upper leaning point of S.*

Proof. If $\alpha = \frac{a}{b}$, the result is straightforward. Otherwise, if $\alpha > \frac{a}{b}$, then l can be written as a linear combination of $l^{\uparrow}$ and a line l_0 of slope $\alpha_0 = \frac{a}{b}$ and intercept β_0, lying in between l_U and l_L. This is easy to see in the dual space representation and illustrated in Figure 3. If $l = (1-t)l_0 + tl^{\uparrow}$ where $t \in [0,1]$, the remainder function $r(\alpha, \beta)$ is equal to $(1-t)r(\alpha_0, \beta_0) + tr(\alpha^{\uparrow}, \beta^{\uparrow})$. The smallest positive value of $r(\alpha^{\uparrow}, \beta^{\uparrow})$ is equal to 0 and reached for the point U_f. Similarly, the smallest positive value of $r(\alpha_0 = \frac{a}{b}, \beta_0)$ is reached for all the upper leaning points of S, thus for U_f. All in all, the smallest positive value of $r(\alpha, \beta)$ is reached for the point U_f. In the same way, the greatest value of $r(\alpha_0 = \frac{a}{b}, \beta_0)$ is reached for all the lower leaning points of S, and the greatest value of $r(\alpha^{\uparrow}, \beta^{\uparrow})$ is reached for the point L', which concludes the proof when α is greater then $\frac{a}{b}$. The case $\alpha < \frac{a}{b}$ is similar, replacing the line $l^{\uparrow}$ by the line $l_{\downarrow}$.

From this property, we deduce that the grid point closest to l and below or on l is an upper leaning point for the DSS minimal characteristics. Similarly, the grid point closest to l and above l is the translation by $(0,1)$ of a lower leaning point for the DSS minimal characteristics. These two points are denoted by U and L respectively.

Consider now the upper convex hull of X and the lower convex hull of $\overline{X}$. Then from 2.2, Proposition 1 and Property 1, the DSS minimal characteristics

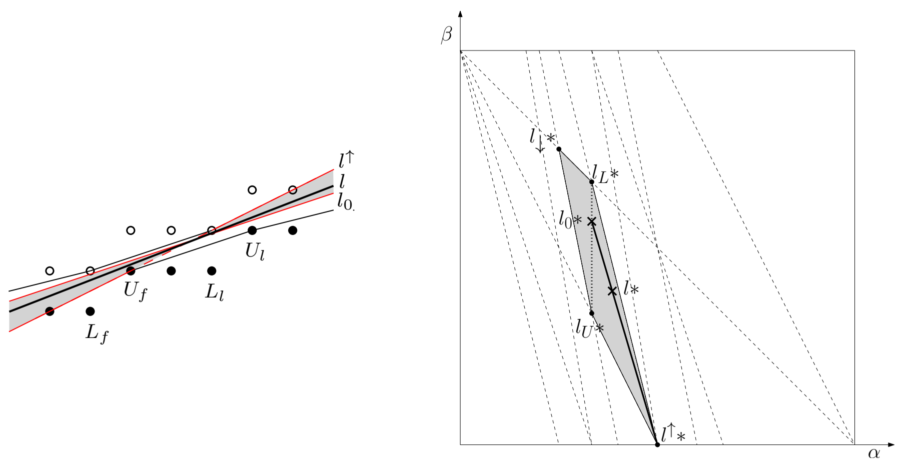

(a) (b)

Figure 3: A separating line l of slope greater than $\frac{a}{b}$ can be written as a linear combination of $l^{\uparrow}$ and a line l_0.

are given by an edge passing through U or L. This leaves us with four edges to check, and the following property is used to conclude.

Property 2. *Consider the two edges e_0 and e_1 of the upper convex hull of $\overline{X}$ passing through U, and the two edges e_2 and e_3 of the lower convex hull of $\overline{X}$ passing through $L + (0, 1)$. We denote by $\frac{a_i}{b_i}$ (with $gcd(a_i, b_i) = 1$) the slopes of these edges. (a, b, μ) are the minimal characteristics of the DSS S if and only if $(a, b) = (a_k, b_k)$ where $b_k = max(b_i)$, and μ is such that the remainder of the DSS (a, b, μ) is equal to 0 on U.*

Proof. From Proposition 1, each edge e_i lies on a line that links either (i) two leaning points, both upper or both lower translated by $(0, 1)$, of the DSS we are looking for, or (ii) one upper leaning point to the translation by $(0, 1)$ of a lower leaning point. The minimal characteristics (a, b) are given by an edge of type (i). Moreover, at most two out of the four edges may lie on the same line, and since there is at most two edges of type (ii), at least one edge is of type (i). If two edges are of type (i), they have the same slope. Since we have no information on the points of the edges apart from U and L, the slopes are used to discriminate between edges of type (i) and edges of type (ii). Indeed, by definition, an edge of type (ii) has a shorter period, i.e. a smallest b_i than an edge of type (i), which concludes the first part of the proof. Once the characteristics (a, b) are known, we just use the fact that U is an upper leaning point of the DSS we are looking for to compute μ and thus end the proof.

3.2. Algorithm

Given a line l and two bounds x_P and x_Q, Properties 1 and 2 directly lead to an algorithm to solve Problem 2 in three steps:

1. compute the upper hull of the grid points X - keep the point closest to l and its two neighbour edges;
2. compute the lower hull of the grid points $\overline{X}$ - keep the point closest to l and its two neighbour edges;
3. among the four edges of slope $\frac{a_i}{b_i}$, the one with maximal b_i gives the solution.

The algorithm of [10] offers a fast solution to solve the first two steps. Indeed, the authors propose an algorithm of complexity $\mathcal{O}(\log(x_Q - x_P))$ to compute the upper and the lower convex hull of the grid points below and above a straight line and between a minimal and maximal abscissa.

In this article, the authors actually mention an algorithm to compute the "reduction" of a straight line over a domain defined by a minimal and a maximal abscissa. The aim is to reduce the coefficients of a straight line digitized over a finite domain. This algorithm is based on the computation of the critical support lines of the convex hulls computed by the algorithm. However, the "reduction" they compute is not equal to the line of minimal characteristics. The first reason is because, as we saw, the critical support lines contain a point of $\overline{X}$. The second reason is given hereafter and illustrated in Figure 4.

If there is no grid point lying exactly on l in the interval $[x_P, x_Q]$ this algorithm computes exactly the hulls we look for (Figure 4 (a)). However, if there exists a point R on l of abscissa $x_P \leq x_R \leq x_Q$, then the lower convex hull computed by this algorithm is erroneous for our purpose: indeed, the computed lower convex hull of $\overline{X}$ contains the point R which is a point of X and not a point of $\overline{X}$ (Figure 4 (b)). To solve this problem, we use the fact that, for a line $l : a_{\mathbf{L}}x - b_{\mathbf{L}}y + \mu_{\mathbf{L}} = 0$ with integer characteristics, there is no grid point lying strictly between l and the line $l' : a_{\mathbf{L}}x - b_{\mathbf{L}}y + \mu_{\mathbf{L}} = 1$. The trick is thus to compute the lower convex hull of the points $\overline{X}$ defined by the line l'.

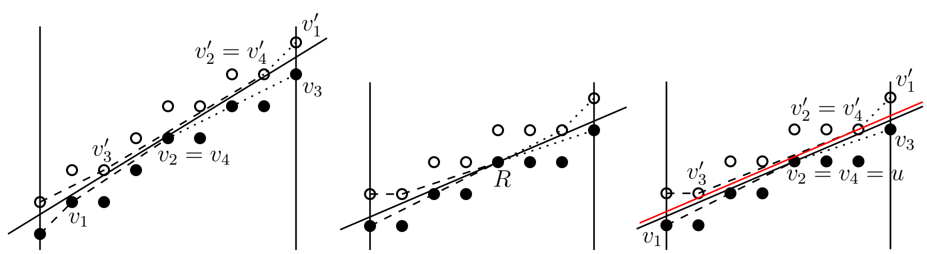

(a) (b) (c)

Figure 4: (a) and (b) Illustration of the algorithm of [10]. In (b), the lower convex hull of $\overline{X}$ contains a point of X. (c) Modification so that the lower convex hull of $\overline{X}$ does not contain a point of X.

As in [10], the upper convex hull of the points X defined by a line l is split in two parts: the left part is composed of the edges of slope greater than the slope of l, while the right part is composed of the edges of slope lower than the slope of l. Then, the computation of the upper convex hull of the points X is completed in two steps, one for each part of the convex hull. Let `localCHLeftRight`$(a_{\mathbf{L}}, b_{\mathbf{L}}, \mu_{\mathbf{L}}, n)$ be Algorithm 1 of [10] for a line $l : a_{\mathbf{L}}x - b_{\mathbf{L}}y + \mu_{\mathbf{L}} = 0$ and abscissas in between 0 and n. This algorithm correctly returns the left part of the upper convex hull of the points X. From this convex hull, we only keep the last two points, the last one being the closest to l.

Algorithm 1: `upperConvexHullOfX`$(a_{\mathbf{L}}, b_{\mathbf{L}}, \mu_{\mathbf{L}}, P, Q)$

---

1 $v_1, v_2 =$ `localCHLeftRight`$(a_{\mathbf{L}}, b_{\mathbf{L}}, r_P, x_Q - x_P)$
$v_1 = v_1 + P$, $v_2 = v_2 + P$
2 $v_3, v_4 =$ `localCHLeftRight`$(a_{\mathbf{L}}, b_{\mathbf{L}}, b_{\mathbf{L}} - r_Q, x_Q - x_P)$
$v_3 = Q + (0,1) - v_3$, $v_4 = Q + (0,1) - v_4$
3 The closest point u is equal to v_2 or v_4
Return $V = (v_1, v_2, v_3, v_4)$ removing multiple copies, and closest point u

---

Algorithm 2: `localCHDSLSubsegment`$(a_{\mathbf{L}}, b_{\mathbf{L}}, \mu_{\mathbf{L}}, P, Q)$

---

1 $V_{inf}, u =$ `upperConvexHullOfX`$(a_{\mathbf{L}}, b_{\mathbf{L}}, \mu_{\mathbf{L}}, P, Q)$
2 $V_{sup} =$ `upperConvexHullOfX`$(a_{\mathbf{L}}, b_{\mathbf{L}}, b_{\mathbf{L}} - r_Q - 1, (0,0), Q - P)$
forall v *in* V_{sup} **do** $v = Q + (0,1) - v$
Let E be the set of edges e, where $e = (v_i, v_{i+1})$ with $v_i \in V_{inf}$ or $v_i \in V_{sup}$
$(b, a) = (0, 0)$
3 **forall** $e(e_x, e_y) \in E$ **do**
  if $e_x > b$ **then** $(b, a) = e$
end
4 $\mu = -au_x + bu_y$
Return (a, b, μ)

Algorithm 1 computes the upper convex hull of the points X lying right below a line l between two points P and Q. r_P (resp. r_Q) stands for the remainder of point P (resp. Q) for the characteristics $(a_{\mathbf{L}}, b_{\mathbf{L}}, \mu_{\mathbf{L}})$. It consists of two calls to `localCHLeftRight` on lines 1 and 2. The call on line 2 corresponds to the computation of the hull from right to left. It returns the ordered list of vertices adjacent to the two edges defined in Property 2 and also remembers the closest point denoted by u on line 3.

Algorithm 2 is the general algorithm to solve Problem 1, rewritten as Problem 2. Lines 1 and 2 compute the upper hull of the points of X and the lower hull of the points of $\overline{X}$ respectively. The result of these calls is illustrated in Figure 4(a) and (c): points v_i are the one returned by the first call to `upperConvexHullOfX` on line 1, whereas the points v'_i are the one returned by the second call on line 2, using the trick presented in the previous paragraph. The loop on line 3 corresponds to the application of Property 2: the edge with maximal x-coordinate defines the sought characteristics.The point u is the point closest to l below l: from Property 1 u is an upper leaning point of the DSS we are looking for and μ is computed from this point on line 4

Concerning the time complexity, algorithm `localCHLeftRight(`$a_{\mathbf{L}}, b_{\mathbf{L}}, \mu_{\mathbf{L}}, n$`)` works in $\mathcal{O}(\log(n))$ from [10], and is called four times. All other operations are done in constant time, so that the complexity of Algorithm `localCHDSLSubsegment` is $\mathcal{O}(\log(n))$ for a subsegment of length n.

4. Fast walk in the Farey fan

This section is dedicated to the presentation of another algorithm to solve Problem 1 using the dual space representation of the set of separating lines.

4.1. Rewriting of the problem

Let us consider all the possible rays $R(x, y)$ as defined in Section 2 with $0 < y \leq x \leq n$. This is equivalent to considering all the linear constraints induced by all the pixels (x, y) such that $0 < y \leq x \leq n$.

Definition 3 (Farey Fan). The Farey Fan of order n, denoted by $\mathcal{F}_n$ is defined in the (α, β) space as the arrangement of all the rays $R(x, y)$ such that $0 \leq y \leq x \leq n$, and such that $0 \leq \alpha \leq 1$ and $0 \leq \beta \leq 1$.

A *facet* of $\mathcal{F}_n$ is a cell of dimension 2 of this arrangement. In the following, a *point* of $\mathcal{F}_n$ stands for any point v of the (α, β) space ($0 \leq \alpha \leq 1$ and $0 \leq \beta \leq 1$) belonging to a ray, and such that the abscissa of v is a fraction of denominator smaller than or equal to n.

If P and Q are respectively the first and last point of the DSS, from the definition and the previous remarks, key Property 3 follows.

Property 3 ([9]). *For any n, there is a bijection between the facets of $\mathcal{F}_n$ and the DSSs of length n (composed of $n+1$ pixels) such that $P = (0, 0)$ and $Q = (n, y_q)$ with $0 < y_q \leq n$.*

Definition 4. Let S be a DSS of length n. $Facet(S)$ is the facet equal to $\mathcal{P}(S)$ in the Farey fan of order n.

Moreover, from Proposition 1 a one-to-one correspondence can be defined between a facet and the characteristic point of the facet.

Definition 5. Let f be a facet of the Farey fan of order n. $CPoint(f)$ is the point v of f such that if $v = (\frac{p}{q}, \frac{r}{q})$, then (p, q, r) are the minimal characteristics of the DSS $Facet^{-1}(CPoint^{-1}(v))$.

The Farey Fan of order 6 is depicted in Figure 5(a). The characteristic point of a few facets is depicted. Note that three types of facets can be identified :

- quadrilateral facets (denoted by Q, in orange in Figure 5(a)) ;
- upper triangular facets (denoted by $T_{\uparrow}$, in green in Figure 5(a)) ;

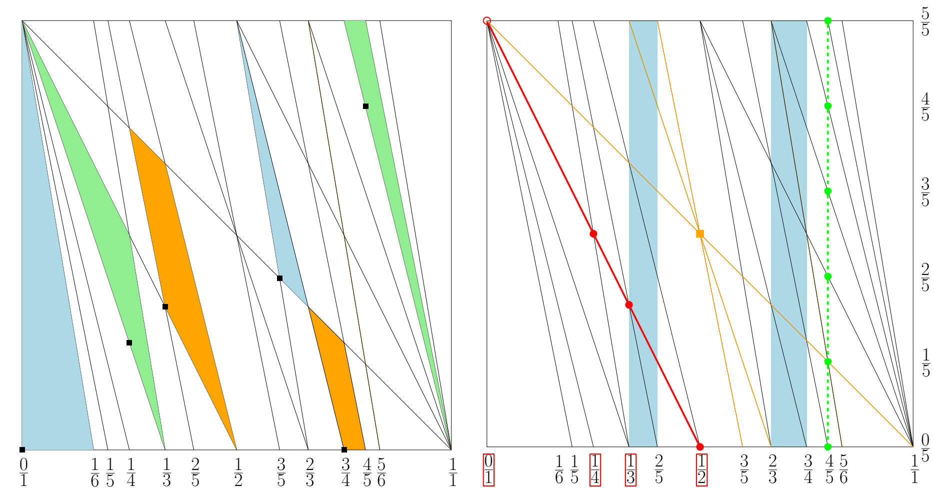

(a) (b)

Figure 5: (a) The Farey Fan of order 6. (b) Illustration of properties 4 to 6.

- lower triangular facets (denoted by $T_\downarrow$, in blue in Figure 5(a)).

Let us now go back to Problem 1. After a translation of the characteristics of $\mathbf{L}$ such that P is set to the origin ($\mu_\mathbf{L} \leftarrow \mu_\mathbf{L} + a_\mathbf{L} x_P - b_\mathbf{L} y_P$), this problem is equivalent to the following one :

Problem 3. Given a point $\mathbf{\Lambda}(\frac{a}{b}, \frac{\mu}{b})$, find the point v of the Farey fan of order $n = x_Q - x_P$ such that $\mathbf{\Lambda} \in CPoint^{-1}(v)$.

In other words, the problem is to find the characteristic point of the facet of $\mathcal{F}_n$ containing $\mathbf{\Lambda}$.

All in all solving Problem 3 is equivalent to performing a point location in an arrangement of lines. However, the number of facets in the Farey fan of order n (which is equal to the number of DSS of length n) is in $\mathcal{O}(n^3)$ [19, 20, 21], and point location algorithms in such a structure are expensive in term of both time and space complexity [22]. This brute force approach is then less efficient than classical DSS recognition algorithms [3, 4, 23, 5].

In the following sections, we revisit the approach proposed by [9] and present an algorithm to solve Problem 3 in time complexity $\mathcal{O}(\log n)$, without explicitly computing the Farey fan. In the next section, we recall several structural and arithmetical properties of the Farey fan, and derive some very useful corollaries. These properties are the core of the algorithm detailed in section 4.3.

4.2. Properties of the Farey Fan

The Farey series of order n is the set of irreducible fractions in $[0, 1]$ of denominator lower than or equal to n [24]. The construction of the Farey series of order n from the Farey series of order $n-1$ is simply done as follows. Consider two consecutive fractions $\frac{p}{q}$ and $\frac{p'}{q'}$ of the Farey series of order n. All the properties below are illustrated in Figure 5(b) in the Farey fan of order 6. The first four properties are from [9] and the reader is invited to consult this reference for the proofs, that are fairly simple.

Property 4 ([9]). *The abscissas of intersections of a ray $R(x, y)$ of $\mathcal{F}_n$ with other rays are* **consecutive terms** *of a Farey series of order* $\max(x, n-x)$.

In Figure 5(b), the abscissas of the intersections between the ray $R(2, 1)$, depicted in red, and the other rays of $\mathcal{F}_6$ are consecutive terms of the Farey series of order $4 = \max(2, 6-2)$.

Property 5 ([9]). *Let f_i and f_{i+1} be two consecutive fractions of the Farey series of order n. In the interval $f_i < \alpha < f_{i+1}$, there is no intersection of rays. Thus, in this interval the Farey fan is a simple* **ladder** *of rungs.*

In Figure 5(b), two ladders are depicted in blue for $f_i = \frac{1}{3}$ and $f_i = \frac{2}{3}$.

Property 6 ([9]). *Let $v(\frac{p}{q}, \frac{r}{q})$, $0 \leq p \leq q \leq n$, be a point of $\mathcal{F}_n$. Let $R(x_0, y_0)$ be the ray of minimum slope passing through v. The other rays passing through v have a slope equal to $x_0 + kq$ with $k \in \mathbb{Z}$ and $x_0 + kq \leq n$.*

In Figure 5(b), three rays go through the point $(\frac{1}{2}, \frac{1}{2})$ (in orange). The slopes of these rays are equal to $x_0 = 1$, 3 and 5. From this property, we can derive the following corollary.

Corollary 1. *Let $v(\frac{p}{q}, \frac{r}{q})$, $0 \leq p \leq q \leq n$, be a point of $\mathcal{F}_n$. Let $R(x, y)$ be a ray passing through p. R is the* ray of smallest slope *passing through v if and only if $x - q < 0$. It is the* ray of greatest slope *passing through v if and only if $x + q > n$.*

The following property is similar to Corollary 1 in [9], but brings in more information.

Property 7. *Let $\frac{p}{q}$ be a fraction of the Farey series of order n. The intersection between the line $\alpha = \frac{p}{q}$ and $\mathcal{F}_n$ is exactly the set of points $(\frac{p}{q}, \frac{r}{q})$ where r takes all the integer values between 0 and q.*

Proof. We study the intersection between $R(x, y)$ defined by the equation $\beta = -\alpha x + y$ and $\alpha = \frac{p}{q}$. We get $\beta = \frac{-px+qy}{q}$. For $0 \leq y \leq x \leq q \leq n$, the quantity $-px + qy$ takes all the integral values in the interval $[|0, q|]$, which ends the proof.

In Figure 5(b), the intersection between $\alpha = \frac{4}{5}$ (depicted in green) and $\mathcal{F}_n$ is the set of points $(\frac{4}{5}, \frac{r}{5})$ with $r \in \mathbb{Z}$, $0 \leq r \leq 5$. Using Properties 5 and 7, we can prove the following result to compute the ray of smallest slope in a given point.

Corollary 2. *Let $v(\frac{p}{q}, \frac{r}{q})$, $0 \leq p \leq q \leq n$, be a point of $\mathcal{F}_n$. Let $\frac{p'}{q'}$ be the fraction following $\frac{p}{q}$ in the Farey series of order n. The ray of smallest slope passing through v is defined by the point v and the point of coordinates $v'(\frac{p'}{q'}, \frac{r'}{q'})$ where r' is such that $\frac{r'}{q'} \leq \frac{r}{q}$ and $\frac{r'+1}{q'} > \frac{r}{q}$.*

PROOF. From Property 5, $\mathcal{F}_n$ is a ladder in the interval $[\frac{p}{q}, \frac{p'}{q'}]$, which means there is no intersection of rays in this interval. From Property 7, all the rays passing through v cut the line of equation $\alpha = \frac{p'}{q'}$ in a point $v'(\frac{p'}{q'}, \frac{r'}{q'})$, $r' \in \mathbb{Z}$, $0 \leq r' \leq q'$. Among all these rays, the ray of smallest slope is the one that passes through the point $v_{max}(\frac{p'}{q'}, \frac{r_{max}}{q'})$ where r_{max} is the maximal value of r' such that $\frac{r'}{q'} \leq \frac{r}{q}$. It remains to prove that the two points v and v_{max} define a ray of $\mathcal{F}_n$. Let x and y respectively be the slope and the intercept of the line defined by v and v_{max}. We have to prove that: i) x and y are integers, ii) x is lower than n. For any r', and from a direct computation, we get $x = \frac{rq'-r'q}{p'q-pq'}$. Since $\frac{p}{q}$ and $\frac{p'}{q'}$ are consecutive fractions of a Farey series, we have $p'q - pq' = 1$ and x is an integer. The same relation is used to show that y is an integer, which proves i). Let us prove ii). From the definition of r_{max} we have $\frac{r}{q} - \frac{r_{max}}{q'} < \frac{1}{q'}$, which is equivalent to $rq' - r_{max}q < q$. Since q is lower than or equal to n, this ends the proof.

Algorithmically, two solutions are possible to compute the ray of smallest slope through a point using Corollary 2: direct computation or dichotomy. With a direct computation, we get $r_{max} = \lfloor \frac{rq'}{q} \rfloor$: r_{max} is the result of the integer division. A dichotomy costs $\mathcal{O}\log(q')$ and is not interesting since integer numbers only are involved.

4.3. Algorithm: a walk in the Farey Fan

Following Problem 3, we look for the characteristic point of the facet containing a given point $\mathbf{\Lambda}(\frac{a}{b}, \frac{r}{b})$. From Proposition 1, Section 4.1 and Property 7 we have the following characterization of the characteristic point.

Property 8. *A point $v(\frac{p_v}{q_v}, \frac{r_v}{q_v})$ is the characteristic point of a facet if and only if:*

1. *either v is the intersection of the two lower edges:*
   (a) *the ray supporting the right lower edge is the one of smallest slope in v;*
   (b) *the ray supporting the left lower edge is the one of greatest slope in v;*
2. *or v is on the unique lower edge and more than one ray passes through the point $(\frac{p_v}{q_v}, \frac{r_v+1}{q_v})$*

As in [9], the algorithm consists of three steps that are detailed in the following sections :

1. Find the ladder to which $\mathbf{\Lambda}$ belongs;
2. Locate the highest ray that lies on or below $\mathbf{\Lambda}$: this ray supports a lower edge of the facet (Section 4.3.2, Algorithm 5);
3. Walk along the ray(s) to determine the characteristic point (Section 4.3.3, Algorithm 6).

4.3.1. Find the ladder

Given a point $\mathbf{\Lambda}(\frac{a}{b}, \frac{\mu}{b})$, finding the ladder to which $\mathbf{\Lambda}$ belongs in $\mathcal{F}_n$ is equivalent to finding the two fractions with a denominator smaller than n closest to $\frac{a}{b}$ (greater and lower). We look for two fractions $f = \frac{p}{q}$ and $g = \frac{p'}{q'}$ such that $q \leq n$, $q' \leq n$, $f \leq \frac{a}{b} \leq g$, and there is no fraction of denominator smaller or equal to n neither between f and $\frac{a}{b}$ nor between $\frac{a}{b}$ and g.

The solution of this problem uses continued fractions representation of the number to be approximated (see [24, 25] for instance for an introduction on continued fractions). The solution of our problem is brought by the following Theorem (stated in [10, 26], with the proof in [27]).

Theorem 1 (as stated in [26]). *Suppose we are required to find the fraction, whose denominator does not exceed n, which most closely approximates, but is no greater than, the quantity $\frac{a}{b}$. If we construct a sequence of fractions containing all the odd principal convergents of $\frac{a}{b}$ with their corresponding intermediate convergents (if such convergents exist), then the fraction we desire is the element of this sequence with the largest denominator no greater than n.*

Thus the fractions we are looking for can be found by searching in the sequence of odd convergents for the greater one, and even convergents for the lower one. A nice geometrical interpretation of the continued fraction of a number was given by Klein in 1895, and can be found in [25] or [28]: if a fraction $\frac{p}{q}$ is represented by the grid point (q, p), then the odd (resp. even) convergents of a number α are the vertices of the lower (resp. upper) convex hull of the grid points lying above (resp. below) the line $y = \alpha x$. In particular, this leads to a very simple geometrical algorithm to compute the convergents of a rational number. This algorithm called `Geometric-GCD` is presented in [28] and has a complexity $\mathcal{O}(\log(\min(a, b))$ for a fraction $\frac{a}{b}$.

In order to compute the closest convergent with a bounded denominator, we use `Geometric-GCD` algorithm and simply add an upper bounding constraint of the form $x \leq n$ as in [10] to get the hybrid Algorithm 3. As in [10], the `Intersection`$(P, \vec{v}, l)$ function computes the intersection point between the straight line defined by the point P and the vector $\vec{v}$, and the straight line l. This point is of the form $P + \alpha\vec{v}$, and the function `Intersection` returns $\lfloor \alpha \rfloor$.

Algorithm 4 implements to computation of the ladder around the fraction $\frac{a}{b}$ in the Farey Fan of order n. If b is greater than n, then it consists in a simple call to the `BoundedGeometricGCD` algorithm. Otherwise, a direct call to the `BoundedGeometricGCD` algorithm would return the fraction $\frac{a}{b}$ for both the lower and the upper fraction, which is not the result sought. However, as shown in Figure 6, since we suppose $b < 2n$, a simple call to `BoundedGeometricGCD` also does the trick.

Algorithm 3: `BoundedGeometricGCD(`l`,`n`)`

l_{right} is the vertical line $x = n$
$L = (1, 0)$
$U = (0, 1)$
$i = 0$ **while** continue **do**
  if *i is even* **then**
    $\alpha 1 =$ `Intersection(`U, L, l`)`, $\alpha 2 =$ `Intersection(`U, L, l_{right}`)`
    $\alpha = min(\alpha 1, \alpha 2)$
    $U = U + \alpha L$
    if *($\alpha = \alpha 2$ or U is on l)* **then** continue = false
  else
    $\alpha 1 =$ `Intersection(`L, U, l`)`, $\alpha 2 =$ `Intersection(`L, U, l_{right}`)`
    $\alpha = min(\alpha 1, \alpha 2)$
    $L = L + \alpha U$
    if *($\alpha = \alpha 2$ or L is on l)* **then** continue = false
end
return L as the lower fraction, U as the greater one.

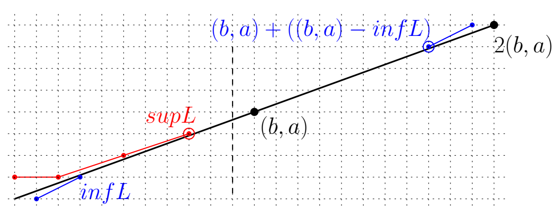

Figure 6: Computation of the ladder when $b \leq n$: the smallest fraction greater than $\frac{a}{b}$ of denominator lower than or equal to n is given by one of the surrounded points.

4.3.2. Locate a lower edge

At this point, we work in a ladder defined by two fractions $f = \frac{p}{q}$ and $g = \frac{p'}{q'}$ of $\mathcal{F}_n$ and $f < g$. This step consists in localising $\mathbf{\Lambda}$ in the ladder by computing the highest ray under $\mathbf{\Lambda}$ in $\mathcal{F}_n$. In [9], this step is performed as a binary search among the rays of the ladder. However, each stage of the binary search requires to solve a Diophantine equation with the extended Euclidean algorithm, reaching a total complexity of $\mathcal{O}(\log^2 n)$.

Our algorithm, presented in Algorithm 5 and illustrated in Figure 7, also performs a dichotomy (line 3), but only on the rays of smallest slope passing through the points of abscissa $\frac{p}{q}$ (in red in Figure 7). The basic operation used in this part is thus the computation of the position of a point $\mathbf{\Lambda}$ with respect to a given ray: the function `PositionWrtRay(point,ray)` returns `on`, `below` or `above`.

Thanks to Property 7, the set of points of abscissa $\frac{p}{q}$ can be defined as on line 1, and the rays of smallest slope are computed in time $\mathcal{O}(1)$ in the ladder using Corollary 2 (line 2). On line 4, the ray of greatest slope is computed from the ray

Algorithm 4: `FindLadder(`$\frac{a}{b}$`,`n`)`

$l : y = \frac{a}{b}x$
if $b > n$ **then**
  $\frac{p}{q}, \frac{p'}{q'}$ = `BoundedGeometricGCD(`l, n`)`
else
  $\frac{p}{q} = \frac{a}{b}$
  $(infL, supL)$ = `BoundedGeometricGCD(`$l, b-1$`)`
  $supR = (b,a) + ((b,a) - infL)$
  if *(supL closer to l than supR) or (the abscissa of supR is greater than n)* **then** $\frac{p'}{q'} \leftarrow supL$ **else** $\frac{p'}{q'} \leftarrow supR$
return $\frac{p}{q}$ and $\frac{p'}{q'}$

of smallest slope thanks to Property 6: its slope is simply equal to $n - (n - x_0) \pmod q$ where x_0 is the slope of the ray of smallest slope. Property 6 is used in line 6. Two solutions are possible: (i) either a dichotomy is performed on the rays passing through v_{j+1}, once again using the function `PositionWrtRay`, (ii) or a direct computation is done. In the case of (ii), let x be the slope of the line passing through v_{j+1} and $\mathbf{\Lambda}$. Let $R_{j+1}(x_{j+1}, y_{j+1})$ be the ray of smallest slope passing through v_{j+1}. Let $[x]$ be the value $x_{j+1} + kq$ nearest to and lower than x, $k \in \mathbb{Z}$: $[x]$ is equal to $\lfloor x \rfloor + x_{j+1} - (\lfloor x \rfloor \pmod q)$ if $\lfloor x \rfloor \neq x_{j+1}$, and equal to x_{j+1} otherwise. If the complexity of solution (i) is straightforwardly logarithmic in the number of rays, which is smaller than q, the complexity of solution (ii) is more complicated to evaluate since it depends on the way floor and modulo functions are implemented. However, we show in Section 4.4 that dichotomy is of help when floating-point input data is considered.

In Figure 7, on the left, the point $\mathbf{\Lambda}$ is located under the ray of greatest slope passing through v_{j+1} (in green, line 5 in Algorithm 5), R_j is returned. On the right, the point $\mathbf{\Lambda}$ is in between the rays passing through v_{j+1}.

4.3.3. Find the characteristic point

Let us denote by M and N the two points defined as the intersection between the ray $R(x,y)$ returned by Algorithm 5 and the vertical lines defining the ladder, i.e. $\alpha = \frac{p}{q}$ and $\alpha = \frac{p'}{q'}$ as defined in Section 4.3.1. The segment $[MN]$ is part of a lower edge of the facet of $\mathcal{F}_n$ containing $\mathbf{\Lambda}$ in $\mathcal{F}_n$.

The first step of the algorithm detailed in Algorithm 6 is to compute the extremities of the lower edge containing $[MN]$. To do so, the key point is to use Property 4 to characterize the points of intersection between a ray and other rays. Given a ray $R(x,y)$ of the Farey Fan $\mathcal{F}_n$ and a point $v(\frac{p}{q}, \frac{r}{q})$ on this ray, v is the crossing point of several rays if and only if $q \leq \max(x, n-x)$. Thus, the abscissa of the left (resp. right) extremity of the lower edge is given by the term of the Farey series of order $\max(x, n-x)$ preceding (resp. following $\frac{p}{q}$ (resp. $\frac{p'}{q'}$) (line 1 of Algorithm 6). This step is simply completed with a call to

Algorithm 5: `localizeLowerEdge`$(\frac{p}{q}, \frac{p'}{q'}, \mathbf{\Lambda})$

Let $v_i = (\frac{p}{q}, \frac{i}{q})$, $i \in \mathbb{Z}$, $0 \leq i \leq q$
Let $R_i(x_i, y_i)$ be the ray of smallest slope passing through v_i
Perform a dichotomy on the R_i to compute $j \in [|0, q-1|]$ such that $\mathbf{\Lambda}$ is above R_j and below R_{j+1}
Let R'_{j+1} be the ray of greatest slope passing through v_{j+1}
if `PositionWrtRay`$(\mathbf{\Lambda}, R'_{j+1})$ = on **then**
  return R'_{j+1}
else
  if `PositionWrtRay`$(\mathbf{\Lambda}, R'_{j+1})$ = below **then**
    return R_j
  else
    Among all the rays passing through v_{j+1}, find the ray R which is right under $\mathbf{\Lambda}$ and **return** R

the function `BoundedGeometricGCD` for the line of slope $\frac{p}{q}$ and with an upper bounding constraint set to $\max(x, n-x)$ (Algorithm 6, line 1). We get the two fractions $\underline{\frac{p}{q}}$ and $\overline{\frac{p}{q}}$ preceding and following $\frac{p}{q}$ in the Farey series of order $\max(x, n-x)$. Note that since $\frac{p}{q}$ and $\frac{p'}{q'}$ are consecutive fractions of the Farey series of order n, the fraction $\overline{\frac{p}{q}}$ is also greater than $\frac{p'}{q'}$. From these two fractions we compute the two points $\underline{O}$ of R with abscissa equal to $\underline{\frac{p}{q}}$ and $\overline{O}$ of R with abscissa equal to $\overline{\frac{p}{q}}$ (line 2).

At this point, $[\underline{O}\overline{O}]$ is a lower edge of the facet containing $\mathbf{\Lambda}$. Then, the three cases illustrated in Figure 8 can occur: either $\underline{O}$ or $\overline{O}$ is the characteristic point (case (a) and (b)), or not (case (c)). We use Property 8 to distinguish between these cases:

- if R is the ray of smallest slope in $\underline{O}$, then $\underline{O}$ is the characteristic point: the condition line 3 refers to Corollary 1;
- if R is the ray of greatest slope in $\overline{O}$, then $\overline{O}$ is the characteristic point: the condition line 4 refers to Corollary 1;
- otherwise, the facet is lower triangular, and the abscissa of the characteristic point is given by the mediant of the abscissas of the lower edge extremities, *i.e.* $\underline{O}$ and $\overline{O}$ (direct consequence of Property 4): on line 5, the mediant is computed, and the point of R with this abscissa is the characteristic point.

4.3.4. General algorithm and Complexity

The general algorithm `FareyFanDSLSubsegment` gathering all the functions presented before is summed up in Algorithm 7. It solves Problem 3, equivalent

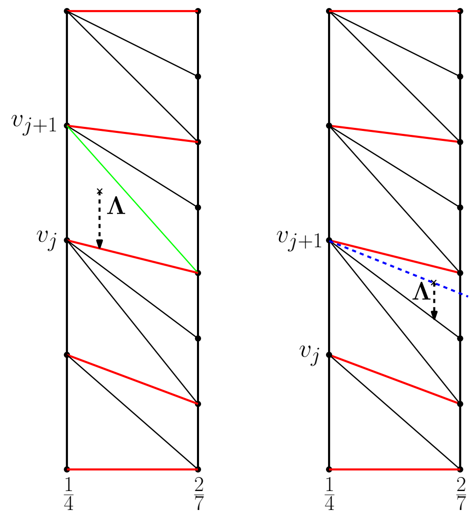

Figure 7: Illustration of Algorithm 5: the dichotomy is performed on the red rays only.

to Problem 1 returning the point of the Farey Fan which is the characteristic point of the DSL subsegment preimage.

Lemma 1. *The complexity of Algorithm 7 is in* $\mathcal{O}(\log(n))$.

PROOF. We assume a computing model where standard arithmetic operations are done in constant time. Finding the ladder is done using Algorithm 4 that has a complexity of $\mathcal{O}(log(n))$.

The localization of a lower edge is done with Algorithm 5: the computation of the R_i (line 2) does not have to be done as a precomputation since the dichotomy (line 3) can be performed on the indices i. Thus they are computed on the fly and only when necessary, and the complexity of these two lines is in $\mathcal{O}(log(q))$ with $q \leq n$. The operations done in lines 4 to 5 are done in constant time. The complexity of line 6 was discussed in Section 4.3.2 and is $\mathcal{O}(\log(q))$ in the worst case. All in all, the complexity of Algorithm 5 is in $\mathcal{O}(\log(q))$.

Algorithm 6 performs the last step of the algorithm. On line 1, computing the points $\underline{O}$ and $\overline{O}$ costs $\mathcal{O}(\log q)$ with $q \leq n$ (see Section 4.3.3). The computation of the mediant fraction on line 5 also has a logarithmic worst time complexity if the fraction is not irreducible. However, we can show that $\underline{p} + \overline{p}$ and $\underline{q} + \overline{q}$ are relatively prime: since $\frac{\underline{p}}{\underline{q}}$ and $\frac{\overline{p}}{\overline{q}}$ are succcessive terms of a Farey series, the denominator of the mediant must be strictly greater than $\max(\underline{q}, \overline{q})$; if $\frac{\underline{p}+\overline{p}}{\underline{q}+\overline{q}}$ was reducible, there would exist an integer $k \geq 2$ such that $\frac{\underline{p}+\overline{p}}{\underline{q}+\overline{q}} = \frac{kp''}{kq''}$, which contradictorily implies $q'' \leq \max(\underline{q}, \overline{q})$. Thus, the mediant computation is done in constant time.

All the other operations of this algorithm take $\mathcal{O}(1)$, which ends the proof.

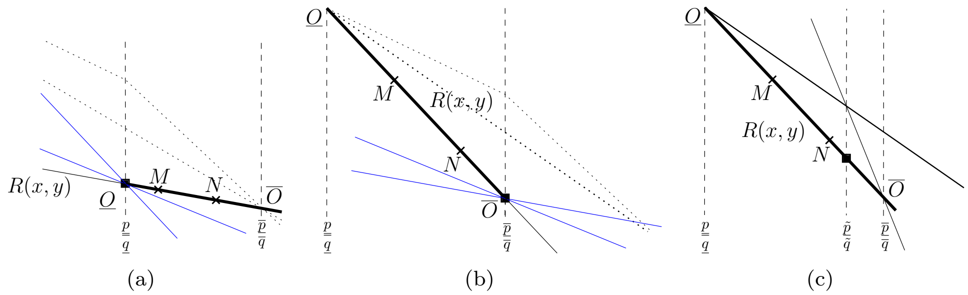

Figure 8: Three cases for the lower edge $[\underline{O}\overline{O}]$: (a) all the rays passing through $\underline{O}$ (in blue) have a slope greater than x and $\underline{O}$ is the characteristic point; (b) all the rays passing through $\overline{O}$ (in blue) have a slope smaller than x and $\overline{O}$ is the characteristic point; (c) neither $\underline{O}$ nor $\overline{O}$ is the solution, and the characteristic point is found with a mediant computation.

Algorithm 6: `findCPoint`$(\frac{p}{q}, \frac{p'}{q'}, R)$

Let $R(x, y)$ be the ray output by Algorithm 5

$(\frac{\underline{p}}{\underline{q}}, \frac{\overline{p}}{\overline{q}}) =$ `BoundedGeometricGCD`$(y = \frac{p}{q}x,\ \max(x, n-x))$

Let $\underline{O}$ (resp. $\overline{O}$) be the intersection point between $\alpha = \frac{\underline{p}}{\underline{q}}$ (resp. $\frac{\overline{p}}{\overline{q}}$) and R

if $x - \underline{q} < 0$ **then**

  return $\underline{O}$ **else**

  if $x + \overline{q} > n$ **then**

    return $\overline{O}$

  else

    Let $\frac{\tilde{p}}{\tilde{q}} = \frac{\underline{p}+\overline{p}}{\underline{q}+\overline{q}}$

    return the intersection point between $\alpha = \frac{\tilde{p}}{\tilde{q}}$ and R

This algorithm solves Problem 3 in $\mathcal{O}(\log(n))$ where n is the order of the Farey fan. From the equivalence of Problems 1 and 3, this algorithm also solves Problem 1 in logarithmic time where n is the length of the DSS.

4.4. Extensions

4.4.1. 4-connected DSL subsegment

In the framework presented above, the DSL and DSS considered are 8-connected sets of pixels. In [8, 1] the authors consider the same problem but with 4-connected digital straight lines and segments. Their definition is similar to the 8-connected lines: a 4-connected DSL of integer characteristics (a, b, μ) is the infinite set of digital points $(x, y) \in \mathbb{Z}^2$ such that $0 \le ax - by + \mu < a + b$ assuming that, as before, $0 \le a \le b$.

Adapting the algorithm `FareyFanDSLSubsegment` for the computation of the minimal characteristics of 4-connected DSL subsegments is actually very easy using the following property.

Algorithm 7: `FareyFanDSLSubsegment`$(a_{\mathbf{L}}, b_{\mathbf{L}}, \mu_{\mathbf{L}}, P, Q)$

Let $\mathbf{\Lambda} = (\frac{a_{\mathbf{L}}}{b_{\mathbf{L}}}, \frac{\mu_{\mathbf{L}}}{b_{\mathbf{L}}})$
Let $n = x_Q - x_P$
$(\frac{p}{q}, \frac{p'}{q'})$ = `FindLadder(`$\frac{a_{\mathbf{L}}}{b_{\mathbf{L}}}$`,`$n$`)`
R = `localizeLowerEdge(`$\frac{p}{q}, \frac{p'}{q'}, \mathbf{\Lambda}$`)`
$CPoint$ = `findCPoint` $(\frac{p}{q}, \frac{p'}{q'}, R)$
return $CPoint$

Property 9. *The grid point $(x+y, y)$ belongs to the 8-connected DSL $(a, b+a, \mu)$ if and only if the grid point (x, y) belongs to the 4-connected DSL (a, b, μ).*

Proof. $(x+y, y)$ belongs to the 8-connected DSL $D(a, b+a, \mu)$ is equivalent to $0 \leq a(x+y) - (b+a)y + \mu < b+a$. Rewriting this equation we get $0 \leq ax - by + \mu < b + a$, which is equivalent to say that (x, y) belongs to the 4-connected DSL (a, b, μ).

Thus, a simple shear transform of matrix $M = \left(\begin{smallmatrix} 1 & 1 \\ 0 & 1 \end{smallmatrix}\right)$ transforms the points of a 4-connected DSL into a 8-connected DSL as illustrated in Figure 9.

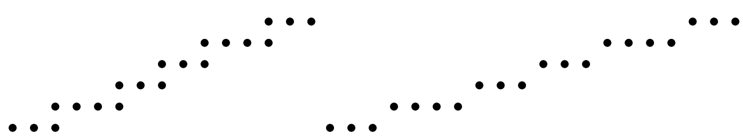

(a) (b)

Figure 9: The 4-connected DSL $(3, 7, 0)$ in (a) is transformed into the 8-connected DSL $(3, 10, 0)$

Consider now Problem 4 which is the same as Problem 1 for 4-connected DSL.

Problem 4. Given a 4-connected DSL L of characteristics $(a_{\mathbf{L}}, b_{\mathbf{L}}, \mu_{\mathbf{L}})$ and two points $P(x_P, y_P)$ and $Q(x_Q, y_Q)$ of this DSL, compute the minimal characteristics (a, b, μ) of the DSS $S = \{(x, y) \in L \mid x_P \leq x \leq x_Q\}$.

Thanks to Property 9, solving Problem 4 is equivalent to solving Problem 1 for a 8-connected DSL of characteristics $(a_{\mathbf{L}}, b_{\mathbf{L}} + a_{\mathbf{L}}, \mu_{\mathbf{L}})$ and the two points $P_t(x_P + y_P, y_P)$ and $Q_t(x_Q + y_Q, y_Q)$. If (a, b, μ) is the solution for Problem 1 on this data, then $(a, b - a, \mu)$ is the solution of Problem 4.

4.4.2. When the DSL characteristics are floating-point numbers

Let us now consider the case when the characteristics of the DSL given as input data are not rational numbers anymore, but real numbers. We now have $\mathbf{\Lambda}(\alpha_{\mathbf{L}}, \beta_{\mathbf{L}})$ with $\alpha_{\mathbf{L}}$ and $\beta_{\mathbf{L}}$ in $\mathbb{R}$.

From a theoretical point of view, the algorithm FareyFanDSLSubsegment proposed in Section 4 works the same. However, as often for geometrical algorithms, things get more complicated when the implementation in concerned. Working on this issue is a research domain by itself, and a huge literature can be found about robustness in geometrical problems. See for instance [29, 30].

Without going to deep in these considerations, we propose a solution to get a robust algorithm for floating-point input data. The robustness is evaluated in Section 5.2.

The only functions that may cause some problems are the ones involving directly the point $\mathbf{\Lambda}(\alpha_{\mathbf{L}}, \beta_{\mathbf{L}})$. A careful analysis of the algorithm shows that this concerns only two particular functions: the function `Intersection(`$P, \vec{v}, l$`)` called in Algorithm 4.3.1 and the function `PositionWrtRay(point,ray)` called on lines 4 and 5 of Algorithm 5. In the first case, the computation of the position of an integer point with respect to a line with floating-point characteristics in involved, while in the second case, the computation of the position of a point with floating-point coordinates with respect to a line with integer characteristics is done. Let us also come back to the line 6 of Algorithm 5. We saw in Section 4.3.2 that two algorithmic choices are possible: either (i) a dichotomy using the function `PositionWrtRay` or (ii) a direct computation involving the computation of the slope of a line going through $\mathbf{\Lambda}$. As we see in the few next lines, it is possible to make the function `PositionWrtRay` robust, while the computation of a slope involving floating-point coordinates plus its rounding seems more difficult to control, on an uncertainty point of view. Thus choice (i) seems to be the better one for floating-point input data.

The uncertainty over the floating-point data is handled in a very classical way using an ε parameter. The way this parameter is used is illustrated in Figure 10. In (a), a centered band of height ε is defined around the line l of the `Intersection(`$P, \vec{v}, l$`)` algorithm. If $P + \alpha\vec{v}$ lies in the gray area, the point is said to be on the line. If it is above the gray area, the point lies above l, and below otherwise. Similarly, in (b) a vertical interval of height ε is defined around $\mathbf{\Lambda}$ in the function `PositionWrtRay`: if the ray R crosses the interval, the point is said to be on the ray, if R is below the interval, R is below l, and above otherwise. We could equivalently have represented the uncertainty around the ray R in (b) as we do in (a), but since the uncertainty is carried by the point $\mathbf{\Lambda}$ we find this representation more accurate.

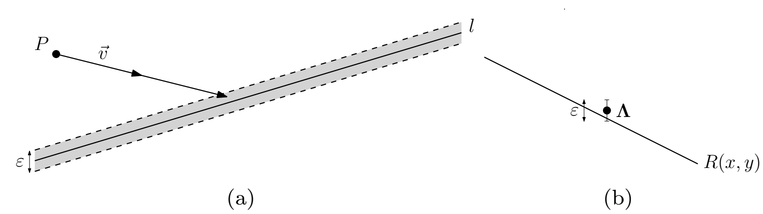

Figure 10: Use of the ε parameter for the `Intersection` (a) and the `PositionWrtRay` (b) functions.

The value of the parameter ε depends on the precision of the input data. If the coordinates of $\mathbf{\Lambda}$ are known with a precision of 10^{-r}, then one can expect that the result of the algorithm on the floating-point point $\mathbf{\Lambda}(\alpha_{\mathbf{L}}, \beta_{\mathbf{L}})$ is the same as the result obtained for the integer characteristics $(a, b, \mu) = (\alpha_{\mathbf{L}}.10^r, 10^r, \beta_{\mathbf{L}}.10^r)$. This suggests that a good value for ε could be 10^{-r}. Indeed, consider a line of equation $l : ax - 10^r y + \mu = 0$, where a and 10^r are relatively prime. Then there is no integer point in the centered band of vertical height $2 * 10^r$. Thus, for instance in the case of the `Intersection` function, any integer point that is in the band of vertical height 10^r is closer from l than from any other line with the same slope and integer characteristics. A similar reasoning can be done for the function `PositionWrtRay`. An experimental validation is conducted in Section 5.2.

Last, we would like to address rapidly the consequences in the case of failures. Concerning the function `PositionWrtRay`, an erroneous answer leads to a bad localization of the lower edge: the result is either the edge below or the edge above the ground truth edge. This means that the final answer will be the characteristic point of the cell just below or just above the ground truth cell. Nevertheless, from the definition of the preimage of a DSS, it is easy to see that the difference between two DSSs the preimage of which share an edge is of exactly one pixel. The abscissa of this pixel is given by the slope of the common edge. This means that an erroneous answer of the function `PositionWrtRay` leads to a difference of at most one pixel between the DSS computed and the ground-truth DSS.

Concerning the function `Intersection`, the analysis is more complicated. Indeed, if the two fractions returned by the function are not consecutive fractions in a Farey series, the algorithm fails to find a solution. If the two fractions are not the correct ones, but are consecutive terms of a Farey series the algorithm will output a result, but the error committed is difficult to estimate. A deeper study could be done if need be.

5. Experimentation

5.1. Implementation and settings

The two algorithms presented in this paper are implemented and available in the generic C++ open-source library `DGtal` [31]. The DGtal library includes several Digital Straight Segment recognition algorithms. Moreover, the authors of [7, 8, 1] made there algorithms available in this library. Comparing our respective results was then an easy and robust task.

To conduct the experiments detailed below, we also reuse the protocol described in [1] and available as a test file in DGtal. The overall protocol is governed by two parameters : N governs the value of b while n is the length of the subsegment. We recall here this protocol that includes a few minor changes.

1. Input characteristics (a, b, μ) are randomly chosen as follows:
    - b is randomly chosen in the interval $[N - \frac{N}{2}, N + \frac{N}{2}]$;

- a is randomly chosen in the interval $[0, b]$ - we also ensure that $gcd(a, b) = 1$;
- μ is randomly chosen in the interval $[0, 2N]$;

2. Points P and Q defining the subsegment are chosen as follows:
   - x_P is randomly chosen in the interval $[0, n]$;
   - x_Q is equal to $x_P + n$ where n is the length of the subsegment;

Concerning the number of draws, we randomly draw 4000 couple of values for b and a, for which 5 values of μ are chosen. For each of the 20000 triplets (a, b, μ), we draw 10 random values for x_P and x_Q.

We repeat this process for values of N equal to 10^k with $k \in [1, 9]$. For each N, the values of n are in the interval $[10, 2N]$ with an increment $n \leftarrow \frac{4}{3}n$. Thus, for each couple of values (N, n) we proceed to $4000 * 5 * 10 = 200000$ draws. The mean computation time of these draws for each couple (N, n) is reported.

As stated in Section 2.3, easy cases are withdrawn: when n gets bigger and close to N, the number of easy cases increases and the mean time would decrease if they were kept, bringing no useful information on the efficiency of the core of the algorithms.

5.2. Experimental correctness

The first experiment is to validate the correctness of the implementation of our two algorithms. To do so, many tests have been conducted. First, the results of the algorithms `FareyFanDSLSubsegment` and `localCHDSLSubsegment` have been directly compared to the results given by the linear-in-time algorithm `ArithmeticalDSS`, as implemented in the DGtal library.

Next, the results of the algorithm `FareyFanDSLSubsegment` in the case of 4-connected DSLs (see Section 4.4) have been compared to the results returned by the algorithm `ReversedSmartDSS`.

Finally, the correctness of the floating-point implementation of the algorithm `FareyFanDSLSubsegment` was also evaluated. To do so, we reused the protocol defined in the previous section, but the possible values of b were powers of 10. For each $b = 10^k$, random integer values of a and μ were chosen. Then the results of the algorithm on the integer data (a, b, μ) and on the floating-point (decimal) data $(\frac{a}{b}, \frac{\mu}{b})$ were compared. In the experiments, the ε parameter was set to 10^k as explained in Section 4.4, and no errors were reported for the several millions of tests carried out.

5.3. General speed contest

The three algorithms `ReversedSmartDSS`, `localCHDSlSubsegment` and `FareyFanDSLSubsegment` all have a theoretical logarithmic time complexity, the logarithm being applied to different values (length of the segment, or difference of depth of the input and output continued fractions). Algorithm `SmartDSS` has a time complexity which depends on the sum of the quotients of the continued fraction of the output slope and on the number of pattern repetitions. In [1], the authors showed that the algorithm SmartDSS was always slower than ReversedSmartDSS. Consequently, for the sake of clarity, we compare our algorithms with ReversedSmartDSS only and try to exhibit in which cases one algorithm may be faster than the others.

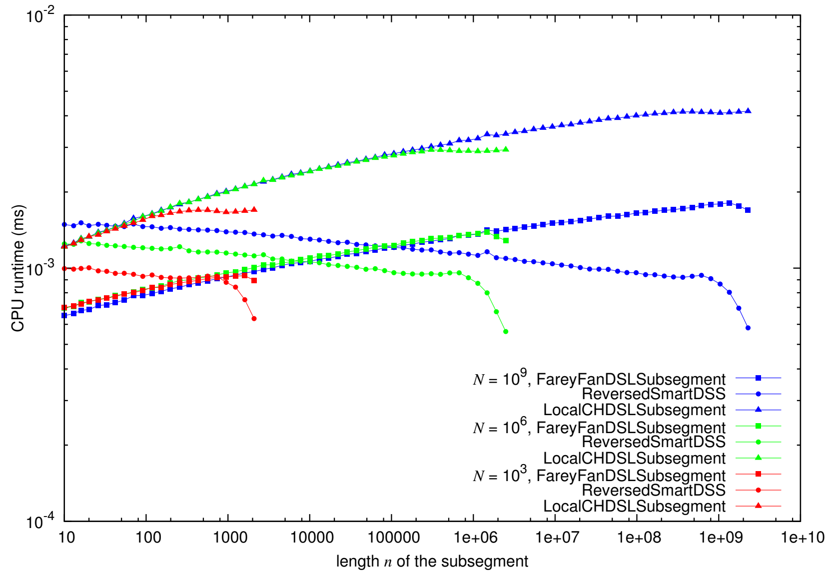

Figure 11: Runtime comparison of our algorithms and one algorithm of [7, 8, 1]

Figure 11 presents the results obtained for three values of N for the three algorithms, for n varying as defined in the previous section. Each value of N is represented by a color (red for 10^3, green for 10^6 and blue for 10^9) and each algorithm is identified by a point type (square for FareyFanDSLSubsegment, disk for ReversedSmartDSS and triangle for localCHDSlSubsegment).

First if we have a look at a particular value of N (one color), we note that FareyFanDSLSubsegment is faster than the other two for small values of n: when n becomes bigger ReversedSmartDSS gets better. For very big values of N and very small n, localCHDSlSubsegment is faster than ReversedSmartDSS but still slower than FareyFanDSLSubsegment.

Next, this graph also brings information about the behaviour of each algorithm for increasing values of N. Algorithms FareyFanDSLSubsegment and localCHDSlSubsegment seem to be insensitive to the value of N for small values of n: for a given n, the computation time is similar for all N. However, in both cases, a slight decrease of the mean computation time occurs when n gets bigger than N.

Concerning the algorithm ReversedSmartDSS, the graph reflects the fact that the complexity depends on both the value of N and the value of n: for a given n, the lower the N, the faster the computation.

To conclude on this experimental study, let us replace this work in the context of image analysis, where the DSS length is bounded by the image size.

Considering that best compact consumer cameras provide 10 megapixels images, the maximal length of DSSs in such images is bounded by a few thousands of pixels. If gigapixel images are considered, the length of the DSSs can reach values of several tens of thousands of pixels, not more for now. In both cases, our algorithm `FareyFanDSLSubsegment` is very competitive for any value of N.

6. Conclusion

We have proposed two algorithms to compute the characteristics of a DSS which is a subsegment of a DSL of known characteristics. These algorithms use two dual representations of the set of separating lines for a given set of grid points. `localCHDSLSubsegment` uses local computation of upper and lower convex hull to find the separating line of minimal characteristics. We provide the theoretical proof that only a few edges of the hulls are necessary to find the result. `FareyFanDSLSubsegment` uses the Farey fan and its numerous arithmetical properties. With this algorithm, the structure of the set of separating lines does not need to be computed since it is known through the Farey Fan, and the problem comes down to a point localization in an arrangement. We also showed that it could be extended to floating-point input data.

Both algorithms have a logarithmic time complexity. Moreover, they are efficient in practice, and easy to implement. The results have been thoroughly compared to existing algorithms, both in terms of correctness of the result (to validate the implementation) and in terms of computation time.

There now exists four algorithms of logarithmic time complexity to solve the DSL subsegment problem. However, no lower bound on the complexity has been proven so far. Is is possible to compute the DSL subsegment minimal characteristics in sub-logarithmic time ? Is it possible in constant time ? This is still an open question.

Another perspective is to use this algorithm in fast digitization algorithms. Suppose we want to digitize a straight segment given by its two floating-point endpoints on a grid of size n. A fast solution could be to compute the minimal characteristics of the DSS before drawing it using the arithmetical DSS definition.

References

[1] J.-O. Lachaud, M. Said, Two efficient algorithms for computing the characteristics of a subsegment of a digital straight line, Discrete Applied Mathematics 161 (15) (2013) 2293–2315.

[2] B. Kerautret, J.-O. Lachaud, Meaningful scales detection along digital contours for unsupervised local noise estimation, Pattern Analysis and Machine Intelligence, IEEE Transactions on 34 (12) (2012) 2379–2392.

[3] I. Debled-Rennesson, J.-P. Reveillès, A linear algorithm for segmentation of digital curves, Inter. Jour. of Pattern Recog. and Art. Intell. 9 (6) (1995) 635–662.

[4] A. Troesch, Interprétation géométrique de l'algorithme d'euclide et reconnaissance de segments, Theor. Comput. Sci. 115 (2) (1993) 291–319.

[5] L. Dorst, A. W. Smeulders, Discrete straight line segments: Parameters, primitives and properties, in: Vision Geometry, series Contemporary Mathematics, Am. Math. Soc., 1991, pp. 45–62.

[6] A. Rosenfeld, R. Klette, Digital straightness: a review, Discrete Applied Mathematics 139 (1-3) (2004) 197–230.

[7] M. Said, J.-O. Lachaud, F. Feschet, Multiscale discrete geometry, in: Discrete Geometry for Computer Imagery, Vol. 5810 of Lect. Notes in Comp. Sci., Springer, 2009, pp. 118–131.

[8] M. Said, J.-O. Lachaud, Computing the characteristics of a subsegment of a digital straight line in logarithmic time, in: Discrete Geometry for Computer Imagery (DGCI), Vol. 6607 of Lecture Notes in Computer Science, Springer, 2011, pp. 320–332.

[9] M. D. McIlroy, A Note on Discrete Representation of Lines, AT&T Technical Journal 64 (2) (1985) 481–490.

[10] E. Charrier, L. Buzer, Approximating a real number by a rational number with a limited denominator: A geometric approach, Discrete Applied Mathematics 157 (16) (2009) 3473 – 3484.

[11] T. Roussillon, Algorithmes d'extraction de modèles géométriques discrets pour la représentation robuste des formes, Ph.D. thesis, Universit Lumire Lyon 2 (2009).

[12] I. Sivignon, Walking in the farey fan to compute the characteristics of a discrete straight line subsegment, in: International Conference on Discrete Geometry for Computer Imagery, Vol. 7749 of Lecture Notes in Computer Science, Springer Berlin Heidelberg, 2013, pp. 23–34.

[13] I. Sivignon, F. Dupont, J.-M. Chassery, Digital intersections : minimal carrier, connectiviy and periodicity properties., Graphical Models 66 (4) (2004) 226–244.

[14] T. Roussillon, L. Tougne, I. Sivignon, Robust decomposition of a digital curve into convex and concave parts, in: 19th International Conference on Pattern Recognition, 2008, pp. 1–4.

[15] L. Dorst, A. N. M. Smeulders, Discrete representation of straight lines, IEEE Transactions of Pattern Analysis and Machine Intelligence 6 (4) (1984) 450–463.

[16] D. Coeurjolly, I. Sivignon, F. Dupont, F. Feschet, J.-M. Chassery, On digital plane preimage structure, Discrete Applied Mathematics 151 (1–3) (2005) 78–92.

[17] J. O'Rourke, An on-line algorithm for fitting straight lines between data ranges, Commun. ACM 24 (9) (1981) 574–578.

[18] B. Hayes, On the Teeth of Wheels, American Scientist 88 (4) (2000) 296–300.

[19] R. Klette, A. Rosenfeld, Digital geometry geometric methods for digital picture analysis, Morgan Kaufmann, 2004.

[20] J. Koplowitz, M. Lindenbaum, A. Bruckstein, The number of digital straight lines on an $n \times n$ grid, IEEE Trans. on Info. Theory 36 (1) (1990) 192 –197.

[21] C. Berenstein, D. Lavine, On the number of digital straight line segments, IEEE Trans. on Pattern Anal. and Mach. Intell. 10 (6) (1988) 880 –887.

[22] R. Wein, E. Fogel, B. Zukerman, D. Halperin, CGAL - 2D Arrangements. URL http://www.cgal.org/Manual/3.3/doc_html/cgal_manual/Arrangement_2/Chapter_main.html

[23] V. Kovalevsky, New definition and fast recognition of digital straight segments and arcs, in: Inter. Conf. on Patt. Anal. and Mach. Intell., 1990, pp. 31 –34 vol.2.

[24] G. H. Hardy, E. M. Wright, An Introduction to the Theory of Numbers, Oxford Society, 1989.

[25] H. Davenport, The Higher Arithmetic: An Introduction to the Theory of Numbers, Cambridge University Press, 1999.

[26] W. Harvey, S. J. C. C, Computing two-dimensional integer hulls, SIAM Journal on Computing 28 (1999) 28–6.

[27] G. Chrystal, Algebra: An Elementary Text-book for the Higher Classes of Secondary Schools and for Colleges, no. vol. 2, Chelsea Publishing Company, 1964.

[28] S. Har-peled, An output sensitive algorithm for discrete convex hulls, Comput. Geom. Theory Appl 10 (1997) 131–136.

[29] L. Kettner, K. Mehlhorn, S. Pion, S. Schirra, C. Yap, Classroom examples of robustness problems in geometric computations, Comput. Geom. Theory Appl. 40 (1) (2008) 61–78.

[30] K. Mehlhorn, C. Yap, Robust Geometric Computation, to appear.

[31] DGtal: Digital Geometry Tools and Algorithms Library. URL http://libdgtal.org